

# Combining Weight Pruning and Knowledge Distillation For CNN Compression

Nima Aghli

Florida Institute of Technology

150 W University Blvd, Melbourne, FL 32901

naghli2014@my.fit.edu

Eraldo Ribeiro

Florida Institute of Technology

150 W University Blvd, Melbourne, FL 32901

eribeiro@fit.edu

## Abstract

*Complex deep convolutional neural networks such as ResNet require expensive hardware such as powerful GPUs to achieve real-time performance. This problem is critical for applications that run on low-end embedded GPU or CPU systems with limited resources. As a result, model compression for deep neural networks becomes an important research topic. Popular compression methods such as weight pruning remove redundant neurons from the CNN without affecting the network’s output accuracy. While these pruning methods work well on simple networks such as VGG or AlexNet, they are not suitable for compressing current state-of-the-art networks such as ResNets because of these networks’ complex architectures with dimensionality dependencies. This dependency results in filter pruning breaking the structure of ResNets leading to an untrainable network. In this paper, we first use the weight pruning method only on a selective number of layers in the ResNet architecture to avoid breaking the network structure. Second, we introduce a knowledge distillation architecture and a loss function to compress the untouched layers during the pruning. We test our method on both image-based regression and classification networks for head-pose estimation and image classification. Our compression method reduces the models’ size significantly while maintaining the accuracy very close to the baseline model.*

## 1. Introduction

Deep-learning algorithms are currently the major producer of state-of-the-art results for computer-vision problems such as object detection [22, 23, 24], image classification [13, 9], and image segmentation [4, 5].

Despite their remarkable accuracy, most state-of-the-art CNNs are both computationally expensive and memory demanding. For instance, deep CNN architectures such as ResNets [9] have millions of parameters that require expensive hardware such as GPUs with a large amount of memory and parallel-computation capabilities if real-time inference

is expected.

Different methods have been proposed to reduce the computational complexity of CNNs while maintaining the compressed network’s accuracy similar to that of the original model. Leng *et al.* [20] proposes a weight quantization algorithm to compress CNNs by quantizing each full-precision weight in the network to a small number of bits. Hinton *et al.* [10] introduces the teacher-student knowledge distillation (KD) method, where a deeper teacher network distills the knowledge of its feature maps to a smaller student network. Additionally, different weight-pruning methods have been proposed [12, 8], where neurons that do not contribute to the model’s prediction are removed.

In this paper, we propose a network-compression method for deep CNNs by combining weight pruning via activation analysis [12] and knowledge distillation. To demonstrate our approach, we apply the compression method to a head-pose estimation regression network and to an image-classification network without any significant loss of accuracy over the original uncompressed network. We also compare inference time of the compressed networks on a PC, embedded GPUs, and embedded ARM CPU. Finally, we compare the compressed head-pose model’s robustness against occlusion, motion-blur, and brightness changes.

## 2. Related Work

Early and shallow networks have been largely outperformed by deeper and wider networks with complex architectures as these networks can capture more complex features. However, most deeper networks suffer from significant redundancy [6] as many network neurons have no contribution to the prediction while still consuming memory and computation. Such redundancy can be reduced by pruning neurons based on their numerical properties. In general, network trimming methods are divided into *connection* and *weight-pruning* categories. Han *et al.* [8] propose a model-compression method as an iterative approach that prunes the connections from the weights with near-zero values followed by weight quantization. Instead of pruning connections, Hu *et al.* [12] propose an iterative neuron pruning

as they show that connection pruning does not bring large improvements on GPUs since convolutional operations in GPUs are converted from 2-D to 1-D vectors followed by matrix multiplication. Hence, when pruning connections instead of neurons, the multiplications stay the same.

Knowledge distillation is another approach to compression that transfers useful feature representation from a teacher network to a student network that has less parameters, and then fine-tunes the student network after knowledge distillation. The teacher-student knowledge-distillation method was first proposed by Hinton *et al.* [10] for classification networks by introducing a distillation loss that uses the softened output of the softmax layer in the teacher network. One of the main challenges with the proposed method was its reduced performance when applied to very deep networks. Additionally, the proposed softened softmax loss was only applicable to classification tasks. To address these issues, Romero *et al.* [25] used an intermediate representation of the teacher model as a hint in addition to the output layer, which improved performance when distilling knowledge from deeper teacher networks. Yim *et al.* [32] applied knowledge distillation to the ResNet architecture by minimizing the L2 loss of Gramian [7] feature matrix in the ResNet modules between teacher and student.

Currently, proposed weight-pruning methods are applied to basic CNN architectures such as AlexNet [19] and VGG [27]. The deeper state-of-the-art models, such as ResNets [9], have complex architectures that limit the application of pruning methods on them. In this paper, we focus on compressing ResNet architectures as they are vastly used in current state-of-the-art classification and regression computer-vision tasks. Our compression method applies to all ResNet-based models.

Our main contributions are threefold: (1) We propose a new weight-pruning strategy for the ResNet architecture inspired by zero-activation pruning [12]. (2) We propose a new knowledge-distillation architecture by using the pruned model as a teacher. (3) We Introduce a new distillation loss to transfer knowledge from the teacher to the student model. Finally, we validate our proposed method by compressing ResNet-based image regression and classification networks.

### 3. Method

Our method has two main steps: 1) Pruning the baseline network by activation analysis to remove neurons that do not contribute to prediction output. 2) Performing knowledge distillation from the pruned (teacher) network to a smaller (student) network to achieve further compression.

#### 3.1. Pruning ResNets with zero activation analysis

As our focus is the real-time inference on GPUs, and neuron pruning has shown effectiveness in reducing

GPU computation, we have employed the iterative weight-pruning method from [12] with some differences. First, Hu *et al.* [12] applies their method to relatively simple and shallow networks such as VGG-16 [27] and LeNet [19]. Instead, we apply pruning to deeper and more complex ResNet architecture. The main challenge with pruning neurons from the ResNets is the dimensionality dependency between some layers to the layers in the previous residual blocks. Residual blocks are the main building parts of ResNets and consist of a residual connection from the previous residual block to the last layer of the current block, followed by an add operation between them. As a result, pruning any layers with such a dependency results in each side of the add operation to have different dimensions and hence, making the model untrainable. Figure 1 shows the internal architecture of two different residual blocks with prunable and un-prunable layers colored in yellow and red, respectively.

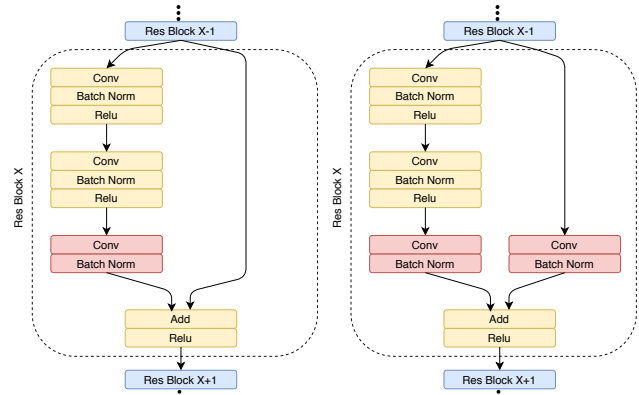


Figure 1. Two different residual blocks in our *ResNet50* model. *Conv* layers in red show un-prunable layers. (left) Residual block with identity connection only. (right) Residual block with additional  $1 \times 1$  convolution for dimensionality reduction.

Second, Hu *et al.* [12] apply pruning to a small number of layers in the model as they point out that pruning too many neurons from multiple layers at one step will reduce the model's performance so much that it cannot be recovered with fine-tuning. In this paper, we show that by skipping unprunable layers in the pruning process, we can remove a large number of filters from multiple layers where the fine-tuning step can recover the model's accuracy on the validation-set to be close to that of the baseline model.

To calculate the importance of any neuron in prunable layers, we calculate the Average Percentage of Zeros (APoZ) [12] for activation output of each neuron for all the samples in the validation-set. Given a prunable layer  $PL_i = \{i = 1, 2, 3, \dots, n\}$ , where  $n$  is the total number of prunable layers in the network, we calculate the importance

of the convolutional filter  $c$  in layer  $i$  as follows:

$$PL_c^{(i)} = \frac{\sum_{k=1}^N \sum_{j=1}^M f(PL_{cj}^{(i)}(k))}{N \times M}, \quad (1)$$

where  $M$  and  $N$  are the total number of validation samples and dimension of the output feature map in the channel  $c$  respectively and  $f$  is calculated as follows:

$$f(\cdot) = \begin{cases} 1, & \text{if } f(PL_{cj}^{(i)}(k)) = 1 \\ 0, & \text{if } f(PL_{cj}^{(i)}(k)) = 0. \end{cases} \quad (2)$$

The pruning process starts by calculating neuron's importance in all prunable layers using Equation 1. If the APoZ of the neuron is larger than the standard deviation of the average APoZs in the same layer, both the neuron and its connections are removed. Once the pruning of all layers is completed, the network is fine-tuned to recover the original accuracy using the baseline model's training configuration. We repeat the process until the network accuracy drops significantly after the iteration.

### 3.1.1 Knowledge distillation from pruned network to student

One of the challenges with the current KD methods is that the number of layers and neurons in the student network is selected arbitrarily. In other words, it is not guaranteed that the student network will not have redundancy in the layers after KD. As a result, the student network can not be considered entirely compressed. We use the pruned model as a teacher instead of the vanilla model in our proposed distillation method. This way, we can ensure that the distillation method will not transfer the student model's possible redundancies. However, as the pruning method could not prune neurons from the un-prunable layers, we reduce the size of those layers in the distillation process by reducing them by a ratio in the student network. As a result, the number of parameters in the student network drops significantly compared to the teacher network.

KD methods that use intermediate layer representation tend to distill the knowledge from the first and the last section of the residual block [7] or use the teacher's middle-layer as a hint [25]. In practice, deeper layers in the network learn the complex features, where the shallow layers learn the simple features. Since the complex features are hard to learn, we distill layer-wise knowledge from the teacher network's last pruned layers and let the student learn the simple features during the KD process. Our proposed approach teaches the student network to minimize the cosine similarity between deep layers and the prediction layer with respect to the teacher's layers. Figure 3 shows the complete architecture of our proposed KD method on ResNet50 network for head-pose estimation.

To distill the knowledge of the teacher's layers to the student's layers, we propose a new loss function. Given a teacher network,  $T$ , and student,  $S$ , we minimize the following distillation loss:

$$CDL = \sum_{i=1}^M \frac{\vec{T}_i \cdot \vec{S}_i}{\|\vec{T}_i\| \|\vec{S}_i\|} + \lambda \frac{\vec{T}_o \cdot \vec{S}_o}{\|\vec{T}_o\| \|\vec{S}_o\|}, \quad (3)$$

where  $M$  is the number of the intermediate KD layers in the teacher network and  $\vec{T}_o$  and  $\vec{S}_o$  is the output layer of the network. For regression network the output vector is regression layer and for classification is the softmax layer.  $\lambda$  is a hyper-parameter to define the importance of the final prediction in last layer over the total loss. In this paper, we set  $M$  to 9 and  $\lambda$  to 1.

Knowledge distillation is a two-step process that starts by freezing the teacher network's layers and feeding a batch of the input samples from the training images to both networks. Then, it calculates the loss based on the distillation loss defined in the Equation 3 and back-propagate the error only on the student network.

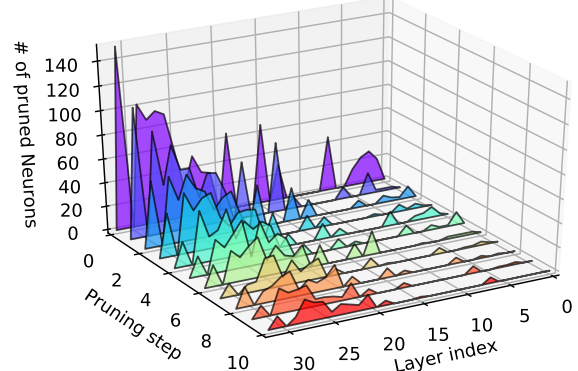


Figure 2. Number of pruned neurons at each step in different layers of the baseline model. Deeper layers show a higher rate of average zero activation larger than 90% during pruning.

## 4. Experiments

We evaluated our compression method on image-based classification and regression networks. For regression, we compressed a 3D head-pose estimation model trained on the ResNet50 [9] network. For classification, we compressed an image-classification network trained on ResNet110 and ResNet164. We used Keras<sup>1</sup> for implementation.

### 4.1. Optimizer

We used the stochastic gradient descent (SGD) [1] with momentum 0.09 for training the baseline networks and fine-tuning the pruned baselines and student networks after

<sup>1</sup><https://keras.io/>

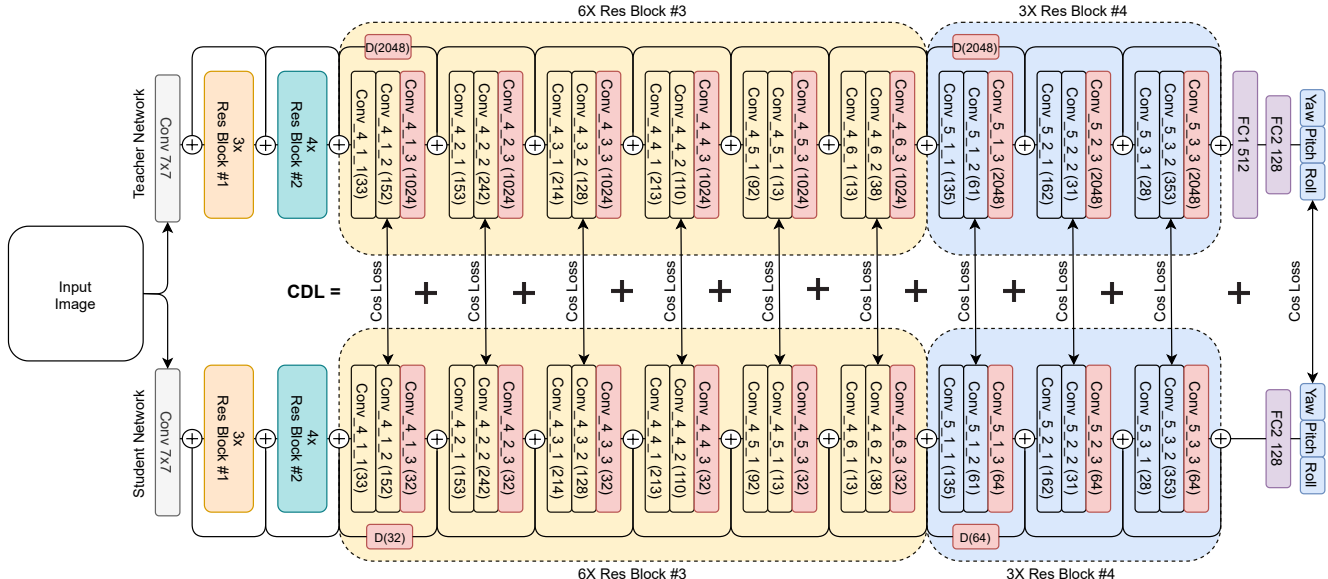


Figure 3. KD architecture of our proposed method. The red layers show the layers that are ignored during the weight pruning process and have the same filter size as the baseline network. The numbers in the parenthesis show the number of filters in each layer. Layers labeled as  $D$  are  $1 \times 1$  dimensionality reduction layers as shown in more details in Figure 1.

knowledge distillation. We used Hyperbolic-Tangent Decay (HTD) [11] as our learning-rate scheduler. For fine-tuning the pruned pose-estimation network at each iteration, we used a learning rate of 0.001 for 20 epochs, and for image classification, we used a learning rate of 0.01 for 200 epochs.

The pose-estimation student network was fine-tuned with a learning rate of 0.1 for 100 epochs, and the student image classifier was fine-tuned with a learning rate of 0.001 for 200 epochs. The end learning-rate in HTD scheduler for all experiments was 0.

We used Adam [15] optimizer with an initial learning rate of 0.1 and scheduling of the learning rates to 0.01, 0.001, 0.0001, and 0.00001 after epoch 20, 45, 55, and 65, respectively, for 85 epochs in the knowledge-distillation process.

## 4.2. Head-pose estimation

The head-pose estimation baseline network was trained on ResNet50 network with two dense layers of size 512 and 128 and a linear layer of size 3 for Yaw, Pitch, and roll estimation at the end of the network. The weights of the network were initialized from the face-recognition network [3]. The input size of the baseline network is  $224 \times 224$  colored images. The baseline was trained on the 300W-LP [33] dataset with image augmentation. All images in the dataset were duplicated and then augmented with random zoom, cropping, and brightness change. For fine-tuning the pruned network at each pruning iteration, we used the same augmented version of 300W-LP and tested on AFLW2000

[33]. The AFLW2000 is a challenging test-set for evaluating head-pose estimation models. It includes ground-truth 3D faces as well as 68 facial-landmarks and head-pose values in yaw, pitch, and roll from the first 2000 images in the AFLW [16] dataset. Unlike the synthesized images in the 300W-LP, the images in the AFLW2000 were gathered from the wild and undergo various illumination and transformations. In addition to testing on AFLW2000, we created three versions of AFLW2000 to test the robustness of the compressed network against motion blur, brightness change, and random cropping of the images as follows:

- **AFLW2000-MB.** Images in the AFLW2000 are convolved with blur kernel of size  $25 \times 25$ .
- **AFLW2000-LB.** The brightness of the images in the AFLW2000 is reduced with the delta value of  $-0.4$ .
- **AFLW2000-OC.** Random rectangular black patches of size  $35 \times 35$  pixels are applied to the images in the AFLW2000. Table 4 shows 3 different examples from augmented versions of AFLW2000.

### 4.3. Results

We pruned the prunable layers from the baseline head-pose estimation network for 16 steps. Figure 2 shows the number of pruned neurons for each layer at each pruning step. The results show that the majority of redundancy in the neurons occurs in the first and deeper layers. After fine-tuning the network in the 16-th step, we use it as a teacher network in our knowledge distillation network.

Table 1. Comparisons with state-of-the-art on AFLW2000.

	Size	Yaw	Pitch	Roll	MAE
Dlib (68 points) [14]	-	23.1	13.6	10.5	15.8
FAN (12 points) [2]	183	6.36	12.3	8.71	9.12
Landmarks [26]	-	5.92	11.86	8.27	8.65
3DDFA [33]	-	5.40	8.53	8.25	7.39
Hopenet [26]	95.9	6.47	6.56	5.44	6.16
SSR-Net-MD [30]	<b>1.1</b>	5.14	7.09	5.89	6.01
FSA-Caps [29]	5.1	4.50	6.08	4.64	5.07
ResNet-50 (Baseline)	99.2	<b>4.38</b>	<b>4.85</b>	<b>3.44</b>	<b>4.22</b>
ResNet-50 (Teacher)	32.6	5.38	5.69	4.19	5.03
ResNet-50 (Student-Distilled)	4.9	5.89	5.63	4.28	5.25
ResNet-50 (Student-Scratch)	4.9	6.95	6.19	4.62	5.90

The student network was initialized with random weights and has the same number of filters in each layer as the teacher network. However, the un-prunable (untouched) layers in the student are divided by 32 in all layers in the student network.

We compared the accuracy, the number of parameters, and the final student model’s size with the state-of-the-art head-pose estimation models trained on the same training/testing protocol.

To show the effectiveness of distilling knowledge from teacher to student, we also trained the same student network without distillation. Table 1 shows the accuracy and compression achieved by our method compared to the state-of-the-art. The results show that our compressed pose-estimation model achieves similar results to the state-of-the-art. However, the network in [29] was trained on images of size  $64 \times 64$  to achieve a smaller model size.

Since we have compressed the network with the input size of  $224 \times 224$  and the larger images represent more information about the subject, the network should perform better against alterations in the input image such as occlusion or motion blur. To make a fair comparison, we tested the augmented version of *AFL2000* on our compressed model and state-of-the-art model [29]. Additionally, we tested the student (Student-DS) network on downsampled to  $64 \times 64$  version of augmented *AFL2000*. Table 2 shows the test results of the student network on the augmented *AFL2000* as well as the downsampled version where our compressed model outperformed [29] in all versions.

#### 4.4. Image Classification

In the second experiment, we used the Cifar10 [17] image-classification dataset. Cifar10 has ten image classes with a total of 50k training and 10k testing images. Here, we trained two ResNet baseline networks (ResNet-110 and ResNet-164) and pruned them for 6 iterations. The pruned networks were used as a teacher in the distillation configuration. The un-prunable layer size was selected in the stu-



Figure 4. Examples of random occlusion, brightness and motion-blur applied to images in AFLW2000.

dent network by dividing their size in the teacher network by 2. The prunable layer size between the teacher and the student remained the same. Table 3 shows the compression result on ResNet-110 and ResNet-164. Our method achieved 4.7 and 3.36 compression rates on ResNet-110 and ResNet-164, respectively while the accuracy only dropped by 1%. Additionally, in Table 4 we compare the compression results on ResNet-110 to different compression methods where the results indicate that our method achieves higher compression rate. Note that in FSNET [31], we only compared to pre-quantization results since weight quantization can be applied to all the networks.

Additionally, we compared our compression method with the TensorFlow Model-Optimization Toolkit (TFMO)<sup>2</sup>. We test all the models on a *ARMv7* processor on a Raspberry Pi2 board.

Table 5 shows a comparison of the baseline model optimized with TFMO and our compression method. While the TFMO archives a  $4 \times$  size and a  $2 \times$  computation efficiency, the accuracy of the optimized model drops significantly. Our compressed model shows significantly better results, while the estimation accuracy stays close to that of the baseline model.

#### 4.5. Inference-time comparison

We compared the inference speed-up achieved by our model-compression approach with the baseline head-pose estimation model. We also compared the results to FSA-Net

<sup>2</sup>[https://www.tensorflow.org/model\\_optimization](https://www.tensorflow.org/model_optimization)

Table 2. Comparisons with state-of-the-art on AFLW2000 with Occlusion, Motion-Blur and Low Brightness.

	Motion Blur			Low Brightness			Random Occlusion		
	FSA-Net [29] Caps-Fusion	Student (ours)	Student-DS (ours)	FSA-Net [29] Caps-Fusion	Student (ours)	Student-DS (ours)	FSA-Net [29] Caps-Fusion	Student (ours)	Student-DS (ours)
Yaw	21.90	<b>12.97</b>	<b>11.56</b>	<b>7.80</b>	8.41	8.75	8.57	<b>8.23</b>	8.62
Pitch	11.07	<b>8.83</b>	<b>8.73</b>	7.28	<b>6.91</b>	<b>7.09</b>	<b>7.87</b>	8.02	8.36
Roll	11.05	<b>7.48</b>	<b>7.12</b>	6.11	<b>5.43</b>	<b>5.65</b>	7.05	<b>6.27</b>	<b>6.4</b>
MAE	14.67	<b>9.76</b>	<b>9.13</b>	7.06	<b>6.91</b>	7.16	7.83	<b>7.5</b>	<b>7.79</b>

Table 3. Compression results on Cifar10

Model	Accuracy	#Params	CR Rate
ResNet-110 (Baseline)	94.27	1.74M	-
ResNet-110 (Teacher)	94.04	0.75M	2.32
ResNet-110 (Student-Distilled)	93.0	0.37M	4.7
ResNet-110 (Student-Scratch)	90.0	0.37M	4.7
ResNet-164 (Baseline)	94.52	2.62M	-
ResNet-164 (Teacher)	94.30	1.44M	1.81
ResNet-164 (Student-Distilled)	93.7	0.72M	3.63
ResNet-164 (Student-Scratch)	89.6	0.72M	3.63

Table 4. Cifar10 compression comparison on state-of-the-art

Model	Accuracy	#Params	CR Rate
ResNet-110 (Baseline)	94.27	1.74M	-
ResNet-110-Student (Ours)	93.0	<b>0.37M</b>	<b>4.7</b>
ResNet-110- Filter pruning [21]	93.30	1.16M	1.5
ResNet-110- FSNET [31]	<b>93.81</b>	0.44M	3.97

Table 5. Comparison between baseline model compressed with our method and TFMO.

Model name	MAE	Size (MB)	Inference(sec)
ResNet-50 (Baseline)	4.77	98 MB	2.5
ResNet-50 (TFMO)	24.4	24.7 MB	1.3
ResNet-50 (Student)(Ours)	5.25	<b>4.9 MB</b>	<b>0.4</b>

since it is the state-of-the-art head-pose estimation model from the accuracy and network complexity perspectives. To further compress our model, we also applied a 16-bit weight quantization [28] to the distilled student model using TensorRT <sup>3</sup>. The test was applied to different PC and low-power embedded GPUs. Table 6 shows the results of running models on different machines where our compressed model achieves the lowest inference time while maintaining the state-of-the-art results on the AFLW2000.

<sup>3</sup><https://developer.nvidia.com/tensorrt>

Table 6. Inference time comparison in seconds.

Model name	GTX1050Ti	Jetson Nano	Jetson Xavier
FSA-Net [29]	0.01	0.08	0.04
ResNet-50 (Baseline)	0.07	0.22	0.03
ResNet-50 (Student)	0.02	0.04	0.02
ResNet-50 (Student)16	<b>0.004</b>	<b>0.008</b>	<b>0.005</b>

## 5. Conclusion

In this paper, we proposed a compression method for network architectures such as ResNets. First, we showed that the ResNet networks' neurons could be pruned only on specific layers. Second, we showed that our knowledge-distillation architecture and loss function reduce the number of weights that could not be pruned due to dimensionality dependencies. Our compression approach works on ResNet-based regression and classification networks.

We used ResNet50 head-pose estimation network for regression tasks. For classification, we used ResNet-110 and ResNet-164. While we achieved similar results in the head-pose estimation network to the state-of-the-art on both model size and accuracy, we showed that our compressed head-pose estimation model outperforms the state-of-the-art on heavily occluded test images. In image classification networks, we achieved similar results to the state-of-the-art accuracy but outperformed on the compression rate.

Finally, as the primary goal of compression is real-time inference on low-end systems, we compared the inference time on multiple embedded GPU and CPU boards. The results presented in this work show the possibility of deploying large Convolutional Neural Networks in low-cost embedded computers for real-world application in the industry.

In this paper, we focused mainly on the ResNet architecture. In future work, we plan to apply the method to different architectures, and also on networks trained on larger image datasets such as Cifar100 [17] and ImageNet [18].

## References

- [1] Léon Bottou. Large-scale machine learning with stochastic gradient descent. In *Proceedings of COMPSTAT'2010*, pages

177–186. Springer, 2010. 3

[2] Adrian Bulat and Georgios Tzimiropoulos. How far are we from solving the 2d & 3d face alignment problem?(and a dataset of 230,000 3d facial landmarks). In *Proceedings of the IEEE International Conference on Computer Vision*, pages 1021–1030, 2017. 5

[3] Q. Cao, L. Shen, W. Xie, O. M. Parkhi, and A. Zisserman. Vggface2: A dataset for recognising faces across pose and age. In *International Conference on Automatic Face and Gesture Recognition*, 2018. 4

[4] Liang-Chieh Chen, George Papandreou, Iasonas Kokkinos, Kevin Murphy, and Alan L Yuille. Semantic image segmentation with deep convolutional nets and fully connected crfs. *arXiv preprint arXiv:1412.7062*, 2014. 1

[5] Liang-Chieh Chen, George Papandreou, Iasonas Kokkinos, Kevin Murphy, and Alan L Yuille. Deeplab: Semantic image segmentation with deep convolutional nets, atrous convolution, and fully connected crfs. *IEEE transactions on pattern analysis and machine intelligence*, 40(4):834–848, 2017. 1

[6] Misha Denil, Babak Shakibi, Laurent Dinh, Marc’Aurelio Ranzato, and Nando De Freitas. Predicting parameters in deep learning. In *Advances in neural information processing systems*, pages 2148–2156, 2013. 1

[7] Leon A Gatys, Alexander S Ecker, and Matthias Bethge. A neural algorithm of artistic style. *arXiv preprint arXiv:1508.06576*, 2015. 2, 3

[8] Song Han, Jeff Pool, John Tran, and William Dally. Learning both weights and connections for efficient neural network. In *Advances in neural information processing systems*, pages 1135–1143, 2015. 1

[9] Kaiming He, Xiangyu Zhang, Shaoqing Ren, and Jian Sun. Deep residual learning for image recognition. In *Proceedings of the IEEE conference on computer vision and pattern recognition*, pages 770–778, 2016. 1, 2, 3

[10] Geoffrey Hinton, Oriol Vinyals, and Jeff Dean. Distilling the knowledge in a neural network. *arXiv preprint arXiv:1503.02531*, 2015. 1, 2

[11] Bo-Yang Hsueh, Wei Li, and I-Chen Wu. Stochastic gradient descent with hyperbolic-tangent decay on classification. In *2019 IEEE Winter Conference on Applications of Computer Vision (WACV)*, pages 435–442. IEEE, 2019. 4

[12] Hengyuan Hu, Rui Peng, Yu-Wing Tai, and Chi-Keung Tang. Network trimming: A data-driven neuron pruning approach towards efficient deep architectures. *arXiv preprint arXiv:1607.03250*, 2016. 1, 2

[13] Andrej Karpathy and Li Fei-Fei. Deep visual-semantic alignments for generating image descriptions. In *Proceedings of the IEEE conference on computer vision and pattern recognition*, pages 3128–3137, 2015. 1

[14] Vahid Kazemi and Josephine Sullivan. One millisecond face alignment with an ensemble of regression trees. In *Proceedings of the IEEE conference on computer vision and pattern recognition*, pages 1867–1874, 2014. 5

[15] Diederik P Kingma and Jimmy Ba. Adam: A method for stochastic optimization. *arXiv preprint arXiv:1412.6980*, 2014. 4

[16] Martin Koestinger, Paul Wohlhart, Peter M Roth, and Horst Bischof. Annotated facial landmarks in the wild: A large-scale, real-world database for facial landmark localization. In *2011 IEEE international conference on computer vision workshops (ICCV workshops)*, pages 2144–2151. IEEE, 2011. 4

[17] Alex Krizhevsky, Geoffrey Hinton, et al. Learning multiple layers of features from tiny images. 2009. 5, 6

[18] Alex Krizhevsky, Ilya Sutskever, and Geoffrey E Hinton. Imagenet classification with deep convolutional neural networks. In *Advances in neural information processing systems*, pages 1097–1105, 2012. 6

[19] Yann LeCun, Léon Bottou, Yoshua Bengio, and Patrick Haffner. Gradient-based learning applied to document recognition. *Proceedings of the IEEE*, 86(11):2278–2324, 1998. 2

[20] Cong Leng, Zesheng Dou, Hao Li, Shenghuo Zhu, and Rong Jin. Extremely low bit neural network: Squeeze the last bit out with admm. In *Thirty-Second AAAI Conference on Artificial Intelligence*, 2018. 1

[21] Hao Li, Asim Kadav, Igor Durdanovic, Hanan Samet, and Hans Peter Graf. Pruning filters for efficient convnets. *arXiv preprint arXiv:1608.08710*, 2016. 6

[22] Wei Liu, Dragomir Anguelov, Dumitru Erhan, Christian Szegedy, Scott Reed, Cheng-Yang Fu, and Alexander C Berg. Ssd: Single shot multibox detector. In *European conference on computer vision*, pages 21–37. Springer, 2016. 1

[23] Joseph Redmon, Santosh Divvala, Ross Girshick, and Ali Farhadi. You only look once: Unified, real-time object detection. In *Proceedings of the IEEE conference on computer vision and pattern recognition*, pages 779–788, 2016. 1

[24] Shaoqing Ren, Kaiming He, Ross Girshick, and Jian Sun. Faster r-cnn: Towards real-time object detection with region proposal networks. In *Advances in neural information processing systems*, pages 91–99, 2015. 1

[25] Adriana Romero, Nicolas Ballas, Samira Ebrahimi Kahou, Antoine Chassang, Carlo Gatta, and Yoshua Bengio. Fitnets: Hints for thin deep nets. *arXiv preprint arXiv:1412.6550*, 2014. 2, 3

[26] Nataniel Ruiz, Eunji Chong, and James M Rehg. Fine-grained head pose estimation without keypoints. In *Proceedings of the IEEE conference on computer vision and pattern recognition workshops*, pages 2074–2083, 2018. 5

[27] Karen Simonyan and Andrew Zisserman. Very deep convolutional networks for large-scale image recognition. *arXiv preprint arXiv:1409.1556*, 2014. 2

[28] Han Vanholder. Efficient inference with tensorrt, 2016. 6

[29] Tsun-Yi Yang, Yi-Ting Chen, Yen-Yu Lin, and Yung-Yu Chuang. Fsa-net: Learning fine-grained structure aggregation for head pose estimation from a single image. In *Proceedings of the IEEE Conference on Computer Vision and Pattern Recognition*, pages 1087–1096, 2019. 5, 6

[30] Tsun-Yi Yang, Yi-Hsuan Huang, Yen-Yu Lin, Pi-Cheng Hsiu, and Yung-Yu Chuang. Ssr-net: A compact soft stage-wise regression network for age estimation. In *IJCAI*, volume 5, page 7, 2018. 5

[31] Yingzhen Yang, Nebojsa Jojic, and Jun Huan. Fsnet: Compression of deep convolutional neural networks by filter summary. *arXiv preprint arXiv:1902.03264*, 2019. 5, 6

[32] Junho Yim, Donggyu Joo, Jihoon Bae, and Junmo Kim. A gift from knowledge distillation: Fast optimization, network minimization and transfer learning. In *Proceedings of the IEEE Conference on Computer Vision and Pattern Recognition*, pages 4133–4141, 2017. [2](#)

[33] Xiangyu Zhu, Zhen Lei, Xiaoming Liu, Hailin Shi, and Stan Z Li. Face alignment across large poses: A 3d solution. In *Proceedings of the IEEE conference on computer vision and pattern recognition*, pages 146–155, 2016. [4](#), [5](#)